Cell Cycle 13:7, 1201–1207; April 1, 2014; © 2014 Landes Bioscience

The aggregation and inheritance of damaged proteins determines cell fate during mitosis

Mary Rose Bufalino[1,*] and Derek van der Kooy[1,2]

[1]Department of Medical Biophysics; University of Toronto; Toronto, Ontario, Canada; [2]Department of Molecular Genetics; University of Toronto; Toronto, Ontario, Canada

Keywords: asymmetric division, Huntington, cell fate, stress, live imaging

Abbreviations: 2-BP, 2-bromopalmitate; ANOVA, analysis of variance; FACS, fluorescence activated cell sorting; Htt, Huntingtin; HD, Huntington disease; GFP, enhanced green fluorescent protein

Recent evidence suggests that proliferating cells polarize damaged proteins during mitosis to protect one cell from aging, and that the structural conformation of damaged proteins mediates their toxicity. We report that the growth, resistance to stress, and differentiation characteristics of a cancer cell line (PC12) with an inducible Huntingtin (Htt) fused to enhanced green fluorescent protein (GFP) are dependent on the conformation of Htt. Cell progeny containing inclusion bodies have a longer cell cycle and increased resistance to stress than those with diffuse Htt. Using live imaging, we demonstrate that asymmetric division resulting from a cell containing a single inclusion body produces sister cells with different fates. The cell that receives the inclusion body has decreased proliferation and increased differentiation compared with its sister cell without Htt. This is the first report that reveals a functional consequence of the asymmetric division of damaged proteins in mammalian cells, and we suggest that this is a result of inclusion body-induced proteasome impairment.

Introduction

Aging is a complex event generally characterized by a decline in function. Recently, a review of the aging literature led to the identification of 9 factors associated with aging, one of which is the loss of proteostasis.[1] In a normal cell, damaged proteins, which have been modified and no longer perform their intended function, are degraded by the proteasome, a multisubunit enzyme complex. Proteasomal activity declines with age in mice, and its role in aging appears to be well conserved, as the mutations of proteasomal components result in reduced lifespan in both mice and yeast.[2,3] The result of proteasomal dysfunction is the accumulation of damaged proteins that can be toxic to the cell, resulting in a decline of function. Both proteins improperly folded and covalently modified as a result of oxidative stress are examples of damaged proteins. As these are post-translational modifications, it is not feasible to overexpress a type of damaged protein in a cell to study its effects. Alternatively, a model of damaged proteins can be used.

Huntington disease (HD) is caused by an abnormal expansion (>40) of cytosine–adenine–guanine repeats in the IT15 gene, which results in the production of abnormal Huntingtin (Htt). HD is characterized by neurodegeneration and Htt aggregates, termed inclusion bodies, both of which increase with age.[4] Similar to damaged proteins, Htt has lost its normal function, can be degraded by the proteasome, forms aggregates, and indirectly impairs proteasomes and decreases a cell's ability to resist stress.[5] For example, Htt expression in yeast with enhanced proteasomal activity results in reduced inclusion body formation compared with wild type.[3] Therefore, Htt provides an excellent model to study the impact of damaged proteins on cells. Initially, inclusion bodies were proposed to be responsible for the neuronal death associated with HD; however, inclusion bodies were not preferentially localized to areas of the brain that experience the greatest cell death during disease[6,7] and did not predict cell death when neurons were tracked with live imaging.[8] This led to the theory that diffuse Htt is the more toxic conformation, and inclusion bodies protect the cell from death by sequestering diffuse Htt,[8] although this is still under debate.[9]

So far, the toxicity of different conformations of Htt primarily has been studied in differentiated cells, as the symptoms of HD result from neuronal death. Cells capable of proliferation also are susceptible to damaged protein toxicity, and it is unclear whether the conformation of damaged proteins determines their toxicity. In contrast to differentiated cells, proliferating cells can reduce damaged protein content through cell division. For example, the polarization of damaged proteins during mitosis results in one cell that is relatively free of damage after division. In *Drosophila*, endogenous damaged proteins have been found to asymmetrically segregate in the female germline stem cell, intestinal stem cell, and larval neuroblast in vivo.[10] Htt aggregates have also been found to polarize during mitosis of embryonic neuroblasts in *Drosophila*.[11] In bacteria and yeast, the unequal inheritance of damaged proteins has been found to have a functional consequence, where the cell that receives the majority of damaged

*Correspondence to: Mary Rose Bufalino; Email: maryrose.bufalino@utoronto.ca
Submitted: 12/16/2013; Revised: 01/29/2014; Accepted: 02/04/2014; Published Online: 02/11/2014
http://dx.doi.org/10.4161/cc.28106

proteins exhibits signs of aging.[12,13] Proteins destined for degradation also have been reported to asymmetrically segregate in mammalian cells in vitro; however, the effect of this phenomenon on cell fate has yet to be described.[14]

To determine the effect of diffuse Htt and inclusion bodies on proliferating cells, we studied the proliferation and resistance to stress of cancer cells expressing inducible Htt fused to GFP. We found that cells containing an inclusion body have reduced proliferation and increased resistance to stress compared to cells with diffuse Htt. Using live imaging, we also demonstrate that cells inheriting the inclusion body during asymmetric division have an increased cell cycle length and tendency to differentiate.

Results and Discussion

Cells containing an inclusion body have a longer cell cycle than cells containing diffuse Htt

Developed from a rat phaeochromocytoma cell line (PC12), 14A2.5 cells express a hybrid ecdysone receptor that allows for inducible expression of Htt containing 103 polyglutamine repeats fused to GFP.[15] After 4 d of induction with 10 μM ponasterone A, 14A2.5 cells were sorted into inclusion body and diffuse populations (**Fig. 1A**; method in ref. 16). Cells were plated in a 96-well plate at 350 cells/well, and their proliferation was assessed over 5 d using the PrestoBlue assay. A 2-way ANOVA demonstrated a significant interaction between cell population and time ($F[8,270] = 11.51$, $P < 0.05$), and Bonferroni post-tests indicated that inclusion body cells had significantly lower proliferation than diffuse and non-induced cells on day 3–5 ($P < 0.05$). There was no significant difference between non-induced and diffuse cells at any time point ($P > 0.05$) (**Fig. 1B**). The average doubling time for non-induced, diffuse, and inclusion body cells were 1.5, 1.6, and 3.0 d, respectively.

Proliferation was also measured after each population was sorted into plates, with a single cell per well. Consistent with the population study, diffuse and non-induced cells had significantly greater proliferation than inclusion body cells over 7 d (**Fig. 1C**, examples in **Fig. 1D**). Average doubling times were nearly identical when cells were plated 350 cells/well or as single cells per well, with times of 1.5, 1.6, and 2.8 d for non-induced, diffuse, and inclusion body single cells, respectively. A 2-way ANOVA demonstrated a significant interaction between cell population and time ($F[12,483] = 2.78$, $P < 0.05$), and Bonferroni post-tests indicated that all populations had significantly different cell numbers on day 7, with inclusion body cells producing the fewest cells over 7 d ($P < 0.05$). Furthermore, only 7.1 ± 2.7% of the wells with inclusion body cells contained a single cell that divided at least once over a 7-d period, whereas the non-induced and inclusion body cells contained dividing cells in 19.0 ± 3.6% and 17.9 ± 4.7% of the wells, respectively. This may be an artifact due to the longer cell cycle time of inclusion body cells and/or cell death. When induced cells were stained for activated caspase 3, there were nearly double the number of inclusion body cells positive for this indicator of apoptosis (11.1 ± 1.1%) compared with diffuse cells (5.9 ± 0.6%). Therefore, cells containing an inclusion body have reduced proliferation and increased cell death compared with cells containing diffuse Htt.

To control for the possibility that cell sorting preferentially changed the growth characteristics of inclusion body cells, proliferation was also assessed upon chemical induction of inclusion bodies in unsorted populations. 2-bromopalmitate (2-BP) reversibly inhibits palmitoylation, which is involved in trafficking Htt to the Golgi and has been shown previously to enhance the formation of inclusion bodies in Htt-expressing cells.[17] When exposed to 2-BP during a 2 d induction period, 73.4 ± 2.2% of cells contained inclusion bodies compared to 14.7 ± 2.9% of cells exposed to induction media only. This difference was also evident when cells were analyzed by FACS (**Fig. 2A**). Analogous to the results of the sorted population growth curve, the population with the greatest number of inclusion bodies (induction + 2-BP) had the slowest doubling time at 2.5 d (**Fig. 2B**). Adding 2-BP to non-induced cultures did not affect the growth rate compared to non-induced cells in growth media; average cell cycle times were 1.8 and 1.9 d, respectively. A 2-way ANOVA demonstrated a significant interaction between cell population and time ($F[12\,400] = 17.33$, $P < 0.05$), and Bonferroni post-tests indicated that induced + 2-BP cells had significantly less proliferation than diffuse and non-induced cells from day 2–5 ($P < 0.05$).

Cells containing an inclusion body are more resistant to stress than cells with diffuse Htt

Currently, it is debated whether inclusion bodies cause the toxic effects of Htt, or if they enhance a cell's ability to protect itself from stress.[18] One hypothesis is that diffuse Htt is toxic, because it disrupts proteasomal function, and inclusion bodies reduce the amount of diffuse Htt within cells through aggregation, thereby limiting their toxic effects.[18] Due to the extensive differences in the diffuse and inclusion body populations, it was predicted that the response to stress would differ as well. When cells were exposed to oxidative stress (hydrogen peroxide) or Doxorubicin (a common chemotherapeutic that causes DNA damage) for 24 h, the cells with the most inclusion bodies (induced + 2-BP) were more resistant than non-induced and induced cells to both

Figure 1 (See opposite page). Inclusion body-containing cells have a longer cell cycle than diffuse cells. (**A**) Htt–GFP expression was induced in 14A2.5 cells with 10 μM of ponasterone-A for 4 d prior to cell suspension and sorting. Cells with inclusion bodies (population P6) can be sorted based on the GFP signal having a smaller height and width than cells containing diffuse GFP throughout the cell (population P7). (**B**) Live non-induced, diffuse, and inclusion body cells were sorted prior to plating at 350 cells/well in maintenance medium in a 96-well plate. The PrestoBlue viability assay was used to assess proliferation for 5 d after plating. PrestoBlue is a resazurin-based compound that is converted into a fluorescent product upon reduction by a viable cell, increasing proportionally with cell number. The graph represents the average of 3 independent experiments and error bars indicate the standard error of the mean. Asterisks indicate a significant difference ($P < 0.05$) in proliferation between inclusion body cells and non-induced and diffuse cells by Bonferroni post-test. (**C**) Non-induced, diffuse, and inclusion body cells were sorted into single cells per well of a 96-well plate. Cells were counted every day for 7 d after plating. The graph represents the average of 3 independent experiments, and error bars indicate the standard error of the mean. Asterisk indicates a significant difference ($P < 0.05$) in proliferation between inclusion body cells and non-induced and diffuse cells by Bonferroni post-test. (**D**) Examples of single-cell proliferation for non-induced (upper), diffuse (middle), and inclusion body cells (lower) (GFP is labeled in green).

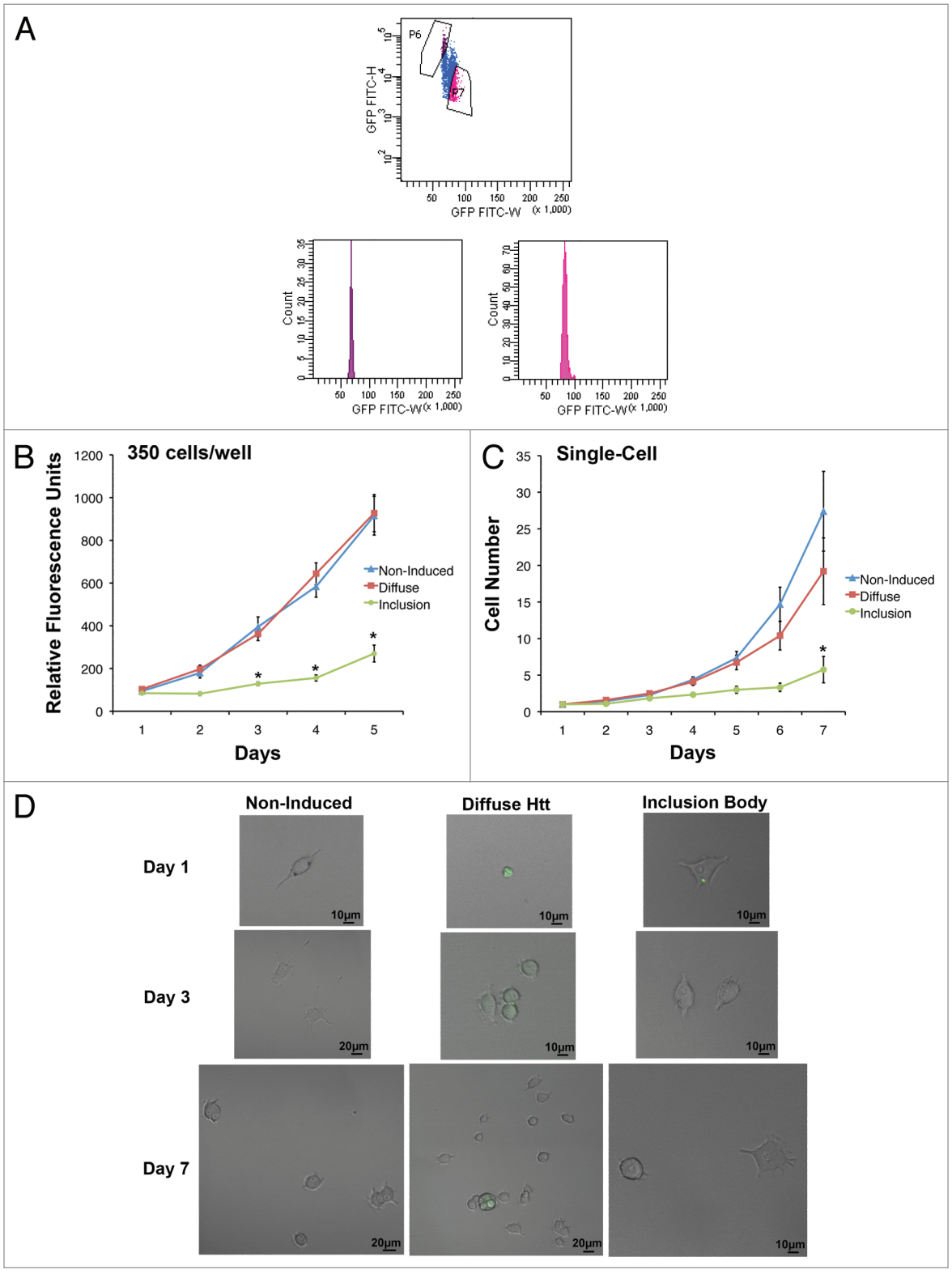

Figure 1. For figure legend, see page 1202.

types of cell stress (**Fig. 2C**, examples **Fig. 2D**). A 2-way ANOVA demonstrated significant main effects of treatment ($F[1,184] = 61.05$, $P < 0.05$) and cell population ($F[3184] = 13.33$, $P < 0.05$). Bonferroni post-tests indicated that adding 2-BP to growth medium did not significantly change the resistance of cells to either type of stress compared to non-induced cells ($P > 0.05$). Cells induced in the presence of 2-BP had a significantly greater ratio of viability (experiment:control) compared to non-induced

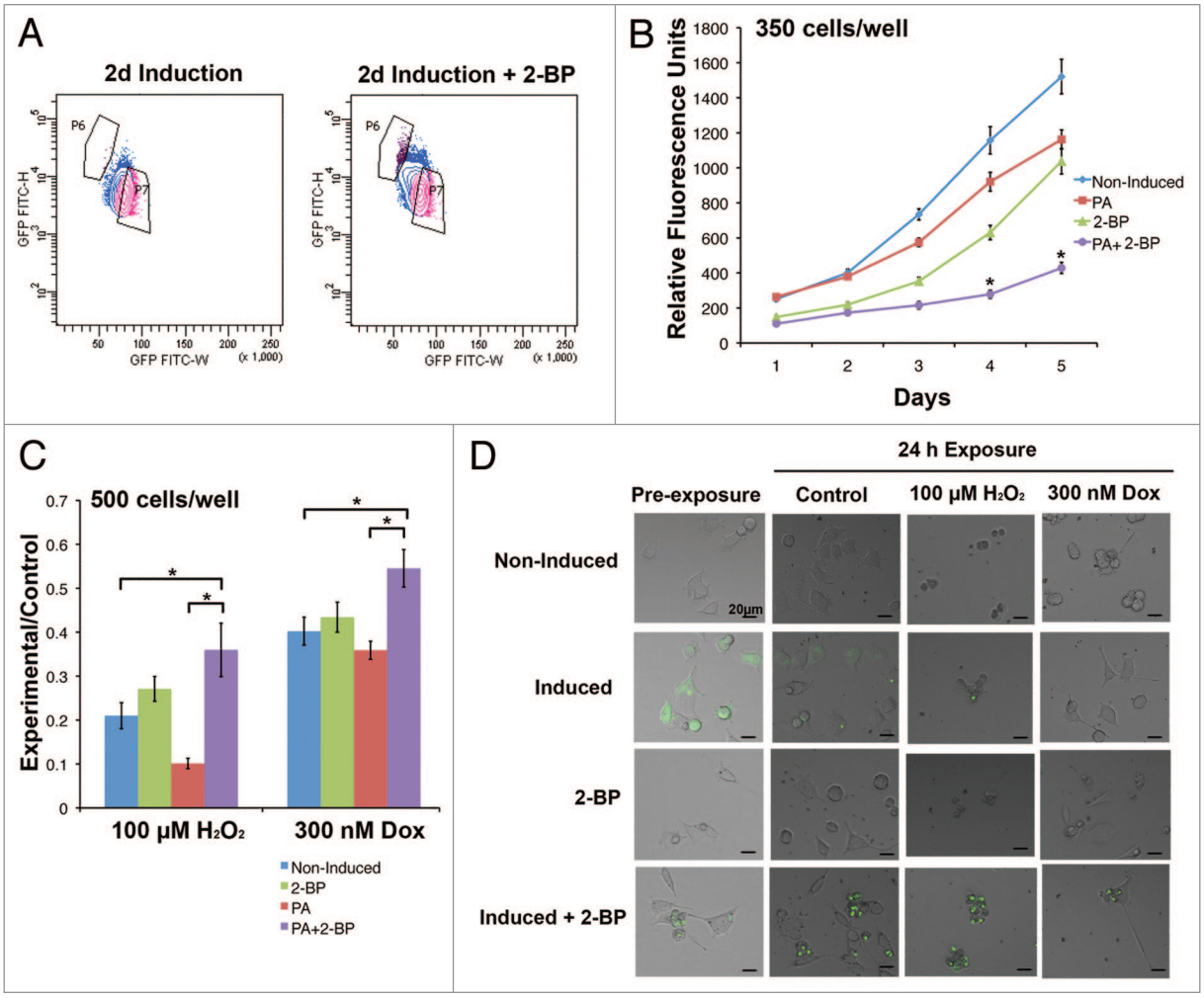

Figure 2. Increasing the number of inclusion body-containing cells by inhibiting palmitoylation increases resistance to stress. (**A**) The population of cells induced in the presence of 2-BP for 2 d has a distinct FACS profile from cells grown in induction medium, revealing an increase in the proportion of the population that contains inclusion bodies (population P6). (**B**) 14A2.5 cells were cultured in maintenance medium (non-induced), induction medium with and without 2-BP, and 2-BP in maintenance medium for 2 d prior to plating at 350 cells/well in 96-well plates in maintenance medium. Cell viability was assessed every day for 5 d after plating. The graph represents the average of 3 independent experiments, and error bars indicate the standard error of the mean. Asterisks indicate a significant difference ($P < 0.05$) in proliferation between cells in the induction + 2-BP condition compared with induced and non-induced cells by Bonferroni post-test. (**C**) To determine if inclusion bodies affect the ability of a cell to resist stress, the same cell populations were plated at 500 cells/well and treated after 24 h of plating with hydrogen peroxide or doxorubicin for 24 h. The PrestoBlue viability assay was used to compare cell viability of control and treated cells, and the ratio of relative fluorescence units in each experimental condition to the same cell type in the maintenance condition is displayed on the *y*-axis. The graph represents an average of 3 independent experiments and error bars indicate the standard error of the mean. Asterisks indicate a significant difference ($P < 0.05$) in ratio of PrestoBlue in experiment:control conditions between cells in the induction + 2-BP condition compared with induced and non-induced cells by Bonferroni post-test. (**D**) Examples of cells in each condition prior to and following treatment (GFP is labeled in green).

and induced cells, indicating a protective effect of inclusion bodies ($P < 0.05$). Therefore, the most slowly cycling cells appear to be the most resistant to stress.

Live-imaging reveals that asymmetric inheritance of inclusion bodies impacts cell fate

Of note, the number of differentiated cells differed between the diffuse and inclusion body-containing cells. Neurite length is often used to measure the differentiation status of PC12 cells,[19] and only 0.8 ± 0.4% of cells induced for 2 d had at least 1 neurite greater than 100 μm in length, whereas 2.6 ± 1.4% of cells exposed to the induced +2-BP condition for 2 d consisted of these differentiated cells 1–2 d after plating. Live imaging was used to determine if the presence of an inclusion body influenced cell differentiation. When inclusion body-containing cells were tracked by live imaging in growth media, no difference was seen in the morphology of the 2 daughter cells (one with an inclusion body and one without) immediately following division. However, there was a difference in the amount of time prior to the next division of the 2 daughter cells. In 81.2% of divisions tracked, the daughter cell containing the inclusion body did not divide or divided after the daughter cell without an inclusion body (example **Fig. 3A**). This lengthening of the cell cycle may be due

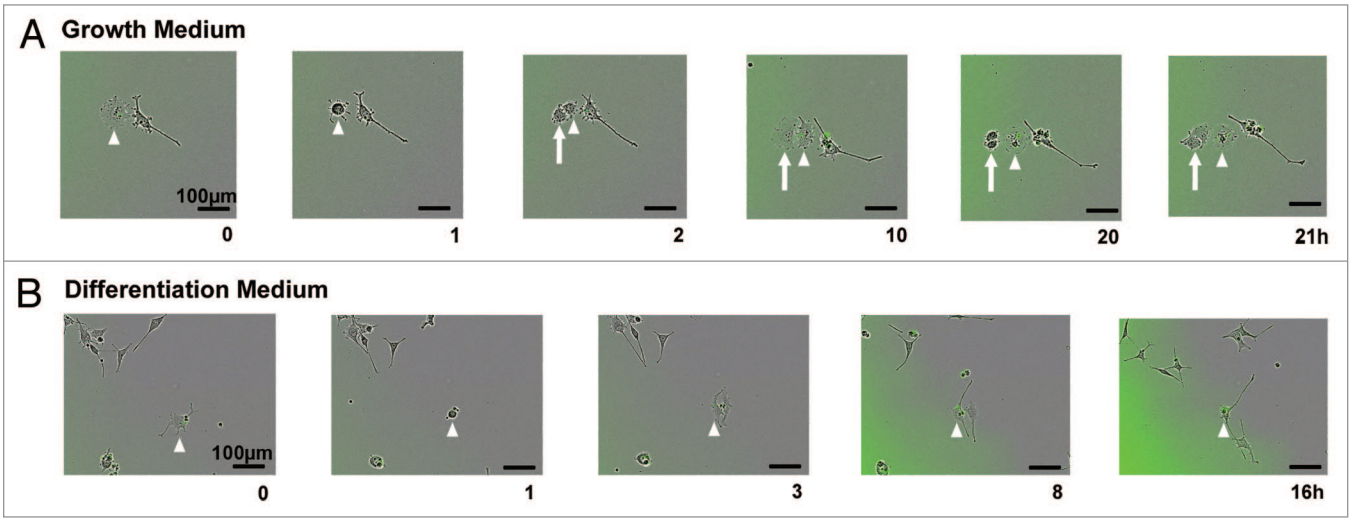

Figure 3. Live imaging reveals differences in cell-fate between progeny of asymmetrically dividing inclusion body cell. (**A**) Example of an inclusion body cell (arrowhead) in maintenance medium that undergoes cell division (GFP is labeled in green). The progeny that does not inherit the inclusion body (arrow) divides before the cell that received the inclusion body (arrowhead) (n = 16). (**B**) Example of an inclusion body cell (arrowhead) in differentiation medium that undergoes cell division (GFP is labeled in green). Neurite length is longer in the cell that inherits the inclusion body (n = 15).

to the time it takes to transport the inclusion body to an area of the cell where it will not interfere with cell division. It is interesting to note that aggregates of hepatitis B virus X protein have been found to lengthen the cell cycle,[20] in contrast to the non-aggregated protein that stimulates proliferation.[21] Therefore, the presence of an aggregate, regardless of the type of protein, may lengthen the cell cycle.

When inclusion body-containing cells were tracked while in differentiation media, there was a clear difference in morphology. In general, when at least one neurite of a cell reaches a length equal to or greater than the diameter of the cell body, the cell is classified as differentiated.[19] After division of inclusion body-containing cells, the daughter cells that received the inclusion body developed significantly longer neurites (average neurite length 109.3 ± 19.9 μm) than the daughter cells without an inclusion body (average neurite length 57.6 ± 11.0 μm) during imaging ($P < 0.05$ by paired 2-tailed Student t test; example **Fig. 3B**). Therefore, the presence of an inclusion body is associated with a longer cell cycle and with enhanced differentiation.

How could an inclusion body influence multiple cell characteristics? We propose that each effect is mediated by a change in the activity of a single complex: the proteasome. Inclusion bodies and proteasome activity are intrinsically linked. Inclusion bodies decrease proteasome activity directly through sequestering components of the proteasome,[22] and indirectly by overloading the capacity of the proteasome.[5] An inhibition of proteasome activity also increases the number of inclusion bodies in Htt-expressing cells.[23] It is interesting to note that a common proteasome inhibitor, lactacystin, was initially characterized as a compound that blocked proliferation and promoted differentiation.[24] Further studies discovered that proteasomal impairment prevents the degradation of factors involved in differentiation.[25] This increases the amount of time that differentiation factors have to correctly localize and generate downstream effectors and is consistent with the cell cycle length hypothesis that emphasizes the importance of longer cell cycle times for differentiation.[26] On the other hand, proliferation depends on the degradation of proteins throughout the cell cycle. For example, Cyclin B promotes the G_2–M transition, and its degradation is required for the cell to exit mitosis.[27] Therefore, cells containing an inclusion body may have enhanced differentiation and reduced proliferation due to proteasomal impairment.

The increased cell cycle length of cells with an inclusion body may also explain their increased resistance to oxidative stress compared with cells with diffuse Htt. A longer cell cycle has been associated with reduced general energy metabolism[28] and, therefore, reduced levels of intracellular ROS, a common by-product of metabolism. Although a population of inclusion body-containing cells is more resistant to extreme stress than a population of cells with diffuse Htt, the small percentage of cells in apoptosis under maintenance conditions was greater in cells containing inclusion bodies. This discrepancy with a previous study, which found an association between cell death and high levels of diffuse Htt but not inclusion body presence in neurons,[8] can be explained by the ability of cells to undergo division in the present study. In maintenance conditions, cells with diffuse Htt rapidly proliferate, which dilutes the level of Htt and any other damaged cellular components. Although the presence of an inclusion body decreases the level of diffuse Htt within cells, their slower rate of cell division prevents them from diluting any toxic by-products of diffuse Htt exposure that may have accumulated before the inclusion body formed, thus leading to higher rates of cell death for proliferating cells with inclusion bodies compared to diffuse Htt. For example, the levels of a toxic product of lipid peroxidation, 4-hydroxy-2-nonenal, have been found to increase in the presence of Htt, and its accumulation may be responsible for increased cell death in inclusion body-containing cells.[29]

Conclusions

Overall, cells containing Htt in a diffuse and inclusion body form are distinct in terms of proliferation, death, resistance to stress, and differentiation. In future studies, it would be interesting to explore the level of proteasome activity in cells with an inclusion body and diffuse Htt to determine if inclusion body-dependent proteasome inhibition is responsible for the decreased proliferation and enhanced differentiation of inclusion body-containing cells. We predict that enhancing proteasome activity in cells with an inclusion body would increase proliferation. Similarly, the removal of an inclusion body from a cell is expected to increase proliferation. One pathway involved in Htt removal is autophagy, where a double membrane surrounds Htt, forming an autophagosome, which then fuses with a lysosome to be degraded.[30] However, it is more difficult to predict if the pharmacological induction of autophagy would alter cell fate in cells containing inclusion bodies. For example, rapamycin inhibits mammalian target of rapamycin (mTOR) activity, which induces autophagy[31] and is involved in maintaining the proliferative potential of cells that experience stimuli inducing cell cycle arrest,[32] yet it appears to be effective at reducing Htt aggregates only in cells with recently formed inclusion bodies.[31] This may be due to inclusion bodies sequestering and inactivating mTOR.[31] Therefore, the ability of rapamycin to restore the proliferation of inclusion body-containing cells may depend on how long an inclusion body is present in a cell and/or the size of the inclusion body. In future studies, it would be interesting to explore the pathways that enhance autophagy and how they affect the proliferation of inclusion body-containing cells.

Materials and Methods

Cell culture

14A2.5 cells were a kind gift from Leslie M Thompson[15] and were maintained in Dulbecco modified Eagle medium, high glucose (DMEM) supplemented with 10% horse serum, 5% fetal bovine serum, 200 μg/mL Zeocin (Invitrogen), and 50 μg/mL Geneticin (Gibco). Htt-GFP expression was induced by adding 10 μM ponasterone A (Invitrogen) to the media for 24 h, 4 d after plating. Cells were grown at 37 °C and 5% carbon dioxide.

Cell sorting

Cells were induced and counterstained with propidium iodide (0.9 μL/mL, Invitrogen) prior to dissociation and sorting using a FacsAria (BD Biosciences). The PulSA method[16] was used to identify cells containing GFP aggregates, which can be differentiated from cells containing diffuse GFP based on a narrower and higher pulse shape.

Aggregate induction

14A2.5 cells were either exposed to maintenance media, 100 μM of 2-BP (Sigma), 10 μM of ponasterone A, or 10 μM of ponasterone A and 100 μM 2-BP 24 h after plating. After 2 d, these cells were dissociated for experiments.

PrestoBlue assay

To assess viability and proliferation 100 μL/mL of PrestoBlue (Invitrogen) was added to each well, and cells were incubated for 1 h in the dark at 37 °C and 5% carbon dioxide. Fluorescence was measured using a SPECTRAmax GEMINI microplate spectrofluorometer (excitation 535 nm, emission 615 nm; Molecular Devices). The average fluorescence of wells containing media only were used to calculate background fluorescence and subtracted from values of wells with cells.

Cell proliferation

Proliferation of cells was measured at a population and single-cell level. Cells were induced and sorted into diffuse, inclusion body, and non-induced populations and plated at 350 cells/well in a 96-well Nunc plate. Proliferation was assessed using the PrestoBlue assay every day for 5 d. Single cells were also plated in a 96-well Nunc plate and the number of cells was counted every day for 7 d.

A similar procedure was used to assess proliferation of cells upon adding 2-BP. Cells in the induced, induced +2-BP, 2-BP, and non-induced conditions were plated at 350 cells/well of a 96-well plate and proliferation was assessed using the PrestoBlue assay every day for 5 d.

Cell cycle length was estimated, assuming exponential growth, based on the following equation: $N(t) = C2^{t/d}$, where N(t) is the relative fluorescence units of PrestoBlue or the number of cells on day 5, d is the doubling time, C is the relative fluorescence units of PrestoBlue or the number of cells on day 1, and t is time.

Immunocytochemistry

Cells were induced for 4 d then plated in maintenance media for 24 h prior to staining. After washing in phosphate buffered saline (PBS), cells were fixed with 4% paraformaldehyde for 30 min at 4 °C. Cells were rinsed 3 times in PBS, prior to blocking in 0.25% Triton X-100 PBS with 5% normal goat serum at 4 °C overnight. Blocking solution was removed, and cells were incubated with rabbit anti-activated caspase 3 (1:200, abcam) in 0.25% Triton X-100 PBS with 1% normal goat serum overnight at 4 °C. After 3 washes with 0.25% Triton X-100 PBS cells were incubated with goat anti-rabbit Alexa Fluor 568 for 3 h at 4 °C. Cells were washed 3 times with 0.25% Triton X-100 PBS prior to staining with Hoescht 33258 (1:1000, Sigma) for 10 min at room temperature. Images were captured at room temperature with the Olympus DP72 12.8 megapixel cooled digital color camera using a 10× (numerical aperture: 0.40) and 20× (numerical aperture: 0.45) objective of a confocal laser scanning microscope (FV1000, Olympus), and any processing with FV1000 software was applied to the whole image.

Stress exposure

Cells exposed to maintenance media, 2-BP, PA, or 2-BP and PA for 2 d were dissociated and plated in maintenance media at 500 cells/well of a 96-well Nunc plate. After 24 h, cells were exposed to DMSO control, 100 μM hydrogen peroxide (Sigma), or 300 nM doxorubicin hydrochloride (BioShop Canada Inc). The PrestoBlue assay was used to measure cell viability 24 h after treatment. Cells were imaged prior to treatment and 24 h after treatment with the FV1000 Olympus confocal microscope described above.

Live imaging

Time-lapse microscopy was performed using an automated Incucyte FLR microscope (Essen Bioscience) with a 10× objective (numerical aperature 1.49). Cells were induced for 4 d and then plated in BD Primaria tissue culture plates (BD Biosciences) with maintenance media or differentiation media (DMEM high

glucose, 1% horse serum, 0.5% fetal bovine serum, 200 μg/mL Zeocin, 50 μg/mL Geneticin, 50 ng/mL nerve growth factor [Invitrogen]) 4 h prior to imaging. Phase-contrast and fluorescence images were captured for 9 fields of view per well of a 6-well plate every hour. Cell divisions were analyzed manually, and ImageJ was used to measure neurite length.

Statistics

A 2-way analysis of variance with Bonferroni post-tests was used to analyze proliferation and stress exposure experiments. A 2-tailed paired Student *t* test was used to compare the length of neurites on sister cells with and without an inclusion body.

Disclosure of Potential Conflicts of Interest

No potential conflicts of interest were disclosed.

Acknowledgments

We thank Leslie Thompson for her generous gift of the 14A2.5 cell line, Pier-Andree Penttila, the flow cytometry technician in the Donnellly Centre, for providing her sorting expertise, and Jason Moffat for sharing his Incucyte. This work was supported by CIHR and NSERC and a Vanier Canada Graduate Scholarship to M.R.B.

References

1. López-Otín C, Blasco MA, Partridge L, Serrano M, Kroemer G. The hallmarks of aging. Cell 2013; 153:1194-217; PMID:23746838; http://dx.doi.org/10.1016/j.cell.2013.05.039
2. Tomaru U, Takahashi S, Ishizu A, Miyatake Y, Gohda A, Suzuki S, Ono A, Ohara J, Baba T, Murata S, et al. Decreased proteasomal activity causes age-related phenotypes and promotes the development of metabolic abnormalities. Am J Pathol 2012; 180:963-72; PMID:22210478; http://dx.doi.org/10.1016/j.ajpath.2011.11.012
3. Kruegel U, Robison B, Dange T, Kahlert G, Delaney JR, Kotireddy S, Tsuchiya M, Tsuchiyama S, Murakami CJ, Schleit J, et al. Elevated proteasome capacity extends replicative lifespan in Saccharomyces cerevisiae. PLoS Genet 2011; 7:e1002253; PMID:21931558; http://dx.doi.org/10.1371/journal.pgen.1002253
4. Cohen A, Ross L, Nachman I, Bar-Nun S. Aggregation of polyQ proteins is increased upon yeast aging and affected by Sir2 and Hsf1: novel quantitative biochemical and microscopic assays. PLoS One 2012; 7:e44785; PMID:22970306; http://dx.doi.org/10.1371/journal.pone.0044785
5. Hipp MS, Patel CN, Bersuker K, Riley BE, Kaiser SE, Shaler TA, Brandeis M, Kopito RR. Indirect inhibition of 26S proteasome activity in a cellular model of Huntington's disease. J Cell Biol 2012; 196:573-87; PMID:22371559; http://dx.doi.org/10.1083/jcb.201110093
6. Gutekunst CA, Li SH, Yi H, Mulroy JS, Kuemmerle S, Jones R, Rye D, Ferrante RJ, Hersch SM, Li XJ. Nuclear and neuropil aggregates in Huntington's disease: relationship to neuropathology. J Neurosci 1999; 19:2522-34; PMID:10087066
7. Kuemmerle S, Gutekunst CA, Klein AM, Li XJ, Li SH, Beal MF, Hersch SM, Ferrante RJ. Huntington aggregates may not predict neuronal death in Huntington's disease. Ann Neurol 1999; 46:842-9; PMID:10589536; http://dx.doi.org/10.1002/1531-8249(199912)46:6<842::AID-ANA6>3.0.CO;2-O
8. Arrasate M, Mitra S, Schweitzer ES, Segal MR, Finkbeiner S. Inclusion body formation reduces levels of mutant huntingtin and the risk of neuronal death. Nature 2004; 431:805-10; PMID:15483602; http://dx.doi.org/10.1038/nature02998
9. Todd TW, Lim J. Aggregation formation in the polyglutamine diseases: protection at a cost? Mol Cells 2013; 36:185-94; PMID:23794019; http://dx.doi.org/10.1007/s10059-013-0167-x
10. Bufalino MR, DeVeale B, van der Kooy D. The asymmetric segregation of damaged proteins is stem cell-type dependent. J Cell Biol 2013; 201:523-30; PMID:23649805; http://dx.doi.org/10.1083/jcb.201207052
11. Rujano MA, Bosveld F, Salomons FA, Dijk F, van Waarde MAWH, van der Want JJL, de Vos RAI, Brunt ER, Sibon OCM, Kampinga HH. Polarised asymmetric inheritance of accumulated protein damage in higher eukaryotes. PLoS Biol 2006; 4:e417; PMID:17147470; http://dx.doi.org/10.1371/journal.pbio.0040417
12. Lindner AB, Madden R, Demarez A, Stewart EJ, Taddei F. Asymmetric segregation of protein aggregates is associated with cellular aging and rejuvenation. Proc Natl Acad Sci U S A 2008; 105:3076-81; PMID:18287048; http://dx.doi.org/10.1073/pnas.0708931105
13. Aguilaniu H, Gustafsson L, Rigoulet M, Nyström T. Asymmetric inheritance of oxidatively damaged proteins during cytokinesis. Science 2003; 299:1751-3; PMID:12610228; http://dx.doi.org/10.1126/science.1080418
14. Fuentealba LC, Eivers E, Geissert D, Taelman V, De Robertis EM. Asymmetric mitosis: Unequal segregation of proteins destined for degradation. Proc Natl Acad Sci U S A 2008; 105:7732-7; PMID:18511557; http://dx.doi.org/10.1073/pnas.0803027105
15. Apostol BL, Kazantsev A, Raffioni S, Illes K, Pallos J, Bodai L, Slepko N, Bear JE, Gertler FB, Hersch S, et al. A cell-based assay for aggregation inhibitors as therapeutics of polyglutamine-repeat disease and validation in Drosophila. Proc Natl Acad Sci U S A 2003; 100:5950-5; PMID:12730384; http://dx.doi.org/10.1073/pnas.2628045100
16. Ramdzan YM, Polling S, Chia CPZ, Ng IHW, Ormsby AR, Croft NP, Purcell AW, Bogoyevitch MA, Ng DCH, Gleeson PA, et al. Tracking protein aggregation and mislocalization in cells with flow cytometry. Nat Methods 2012; 9:467-70; PMID:22426490; http://dx.doi.org/10.1038/nmeth.1930
17. Yanai A, Huang K, Kang R, Singaraja RR, Arstikaitis P, Gan L, Orban PC, Mullard A, Cowan CM, Raymond LA, et al. Palmitoylation of huntingtin by HIP14 is essential for its trafficking and function. Nat Neurosci 2006; 9:824-31; PMID:16699508; http://dx.doi.org/10.1038/nn1702
18. Arrasate M, Finkbeiner S. Protein aggregates in Huntington's disease. Exp Neurol 2012; 238:1-11; PMID:22200539; http://dx.doi.org/10.1016/j.expneurol.2011.12.013
19. Das KP, Freudenrich TM, Mundy WR. Assessment of PC12 cell differentiation and neurite growth: a comparison of morphological and neurochemical measures. Neurotoxicol Teratol 2004; 26:397-406; PMID:15113601; http://dx.doi.org/10.1016/j.ntt.2004.02.006
20. Song C-Z, Bai Z-L, Song C-C, Wang Q-W. Aggregate formation of hepatitis B virus X protein affects cell cycle and apoptosis. World J Gastroenterol 2003; 9:1521-4; PMID:12854155
21. Benn J, Schneider RJ. Hepatitis B virus HBx protein deregulates cell cycle checkpoint controls. Proc Natl Acad Sci U S A 1995; 92:11215-9; PMID:7479968; http://dx.doi.org/10.1073/pnas.92.24.11215
22. Gil JM, Rego AC. Mechanisms of neurodegeneration in Huntington's disease. Eur J Neurosci 2008; 27:2803-20; PMID:18588526; http://dx.doi.org/10.1111/j.1460-9568.2008.06310.x
23. Waelter S, Boeddrich A, Lurz R, Scherzinger E, Lueder G, Lehrach H, Wanker EE. Accumulation of mutant huntingtin fragments in aggresome-like inclusion bodies as a result of insufficient protein degradation. Mol Biol Cell 2001; 12:1393-407; PMID:11359930; http://dx.doi.org/10.1091/mbc.12.5.1393
24. Fenteany G, Schreiber SL. Lactacystin, proteasome function, and cell fate. J Biol Chem 1998; 273:8545-8; PMID:9535824; http://dx.doi.org/10.1074/jbc.273.15.8545
25. Ito Y, Fukushima H, Katagiri T, Seo Y, Hirata S, Zhang M, Hosokawa R, Jimi E. Lactacystin, a proteasome inhibitor, enhances BMP-induced osteoblastic differentiation by increasing active Smads. Biochem Biophys Res Commun 2011; 407:225-9; PMID:21377449; http://dx.doi.org/10.1016/j.bbrc.2011.03.003
26. Calegari F, Huttner WB. An inhibition of cyclin-dependent kinases that lengthens, but does not arrest, neuroepithelial cell cycle induces premature neurogenesis. J Cell Sci 2003; 116:4947-55; PMID:14625388; http://dx.doi.org/10.1242/jcs.00825
27. Reed SI. Ratchets and clocks: the cell cycle, ubiquitylation and protein turnover. Nat Rev Mol Cell Biol 2003; 4:855-64; PMID:14625536; http://dx.doi.org/10.1038/nrm1246
28. Essers MA, Trumpp A, Trumpp A. Targeting leukemic stem cells by breaking their dormancy. Mol Oncol 2010; 4:443-50; PMID:20599449; http://dx.doi.org/10.1016/j.molonc.2010.06.001
29. Lee J, Kosaras B, Del Signore SJ, Cormier K, McKee A, Ratan RR, Kowall NW, Ryu H. Modulation of lipid peroxidation and mitochondrial function improves neuropathology in Huntington's disease mice. Acta Neuropathol 2011; 121:487-98; PMID:21161248; http://dx.doi.org/10.1007/s00401-010-0788-5
30. Luzio JP, Pryor PR, Bright NA. Lysosomes: fusion and function. Nat Rev Mol Cell Biol 2007; 8:622-32; PMID:17637737; http://dx.doi.org/10.1038/nrm2217
31. Ravikumar B, Vacher C, Berger Z, Davies JE, Luo S, Oroz LG, Scaravilli F, Easton DF, Duden R, O'Kane CJ, et al. Inhibition of mTOR induces autophagy and reduces toxicity of polyglutamine expansions in fly and mouse models of Huntington disease. Nat Genet 2004; 36:585-95; PMID:15146184; http://dx.doi.org/10.1038/ng1362
32. Leontieva OV, Lenzo F, Demidenko ZN, Blagosklonny MV. Hyper-mitogenic drive coexists with mitotic incompetence in senescent cells. Cell Cycle 2012; 11:4642-9; PMID:23187803; http://dx.doi.org/10.4161/cc.22937